Chinese Journal of Catalysis 72 (2025) 314–322

available at www.sciencedirect.com

ScienceDirect

journal homepage: www.sciencedirect.com/journal/chinese-journal-of-catalysis

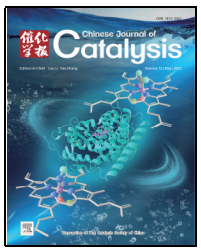

Article

Efficient carbon integration of CO_2 in propane aromatization over acidic zeolites

Cheng Li [a,b], Xudong Fang [a,*], Bin Li [a,b], Siyang Yan [c], Zhiyang Chen [a], Leilei Yang [a,b], Shaowen Hao [a,b], Hongchao Liu [a], Jiaxu Liu [c,*], Wenliang Zhu [a,*]

[a] *National Engineering Research Center of Lower-Carbon Catalysis Technology, Dalian Institute of Chemical Physics, Chinese Academy of Sciences, Dalian 116023, Liaoning, China*

[b] *University of Chinese Academy of Sciences, Beijing 100049, China*

[c] *State Key Laboratory of Fine Chemicals, Frontier Science Center for Smart Materials, School of Chemical Engineering, Dalian University of Technology, Dalian 116012, Liaoning, China*

ARTICLE INFO

Article history:
Received 24 January 2025
Accepted 26 March 2025
Available online 20 May 2025

Keywords:
CO_2 utilization
Propane aromatization
Coupling effect
Acidic zeolites
Lactone

ABSTRACT

Direct converting carbon dioxide (CO_2) and propane (C_3H_8) into aromatics with high carbon utilization offers a desirable opportunity to simultaneously mitigate CO_2 emission and adequately utilize C_3H_8 in shale gas. Owing to their thermodynamic resistance, converting CO_2 and C_3H_8 respectively remains difficult. Here, we achieve 60.2% aromatics selectivity and 48.8% propane conversion over H-ZSM-5-25 *via* a zeolite-catalyzing the coupling of CO_2 and C_3H_8. Operando dual-beam FTIR spectroscopy combined with ^{13}C-labeled CO_2 tracing experiments revealed that CO_2 is directly involved in the generation of aromatics, with its carbon atoms selectively embedded into the aromatic ring, bypassing the reverse water-gas shift pathway. Accordingly, a cooperative aromatization mechanism is proposed. Thereinto, lactones, produced from CO_2 and olefins, are proven to be the key intermediate. This work not only provides an opportunity for simultaneous conversion of CO_2 and C_3H_8, but also expends coupling strategy designing of CO_2 and alkanes over acidic zeolites.

1. Introduction

Carbon dioxide (CO_2), a primary contributor to the greenhouse effect, has been widely recognized as a key driver of pressing environmental challenges [1–3]. Nevertheless, owing to its wide availability and low cost, CO_2 is increasingly regarded as a promising C1 feedstock for the synthesis of value-added chemical products [4–6]. Currently, the utilization of CO_2 to synthesize urea, carbonates and carboxylic acid has been successfully commercialized but with small market demand [7–10]. Olefins or aromatics as bulk chemicals can also be produced from CO_2 hydrogenation which has garnered substantial attention [5,11–14]. Nevertheless, realizing efficient and sustainable CO_2 conversion into aromatics remains a formidable challenge resulting from its high thermodynamic stability ($\Delta_f G^0$ = −396 kJ/mol).

Given the hydrogen cost and product demand, the transformation of CO_2 and hydrogen-rich compounds such as pro-

* Corresponding author. E-mail: xdfang@dicp.ac.cn (X. Fang), liujiaxu@dlut.edu.cn (J. Liu), wlzhu@dicp.ac.cn (W. Zhu).

This work was supported by the National Natural Science Foundation of China (22402179, 22472016, 21991094, 21991090), the "Transformational Technologies for Clean Energy and Demonstration", Strategic Priority Research Program of the Chinese Academy of Sciences (XDA21030100), the Dalian High Level Talent Innovation Support Program (2017RD07), and the National Special Support Program for High Level Talents (SQ2019RA2TST0016).
https://doi.org/10.1016/S1872-2067(25)64680-8

pane (C_3H_8) into aromatics, especially benzene-toluene-xylene (BTX) is an ideal and efficient strategy. Recent studies on CO_2-involved C_3H_8 aromatization have primarily centered on metal-containing catalytic systems [15–20], where CO_2 is typically converted to CO *via* the reverse water-gas shift (RWGS) reaction, thereby facilitating the aromatization process by shifting the reaction equilibrium. This results in suboptimal atom economy and limits the role of CO_2 to a hydrogen management agent rather than a true carbon donor. Overcoming this limitation requires a paradigm shift: from using CO_2 as a facilitator to integrating it as an active reactant in the formation of desired products.

In our previous research, we demonstrated that the coupling conversion of CO_2 and light alkane (C_4–C_6) [21,22] or chloromethane [23] to aromatics can be achieved over acidic zeolites. Remarkably, the novel aromatization mechanism has been proposed including the formation of lactones and cyclopentenone. Thereinto, the carbon atom of CO_2 was incorporated into desired product. However, compared with C_4–C_6 alkanes, the conversion of C_3H_8 is more difficult due to its high bond energy. For example, butanes are converted approximately 4 times faster than C_3H_8 [24]. Therefore, achieving the efficient conversion of C_3H_8 and CO_2 to aromatics is highly challenging. Currently, our group confirmed that the C_3H_8-CO_2 coupling conversion to aromatics can be achieved over Ga/ZSM-5 [25]. The $[GaH_2^+]$/$[GaH^+]$ species have been reported to activate CO_2 and promote its synergistic conversion with propane. Despite this, limited efforts have been devoted to investigating CO_2-C_3H_8 coupling aromatization over acidic zeolite.

In this work, we propose an effective approach for the co-conversion of CO_2 and C_3H_8 into aromatics by coupling hydrogen-deficient and hydrogen-rich species over acidic zeolites. Under reaction conditions of 723 K, 3.0 MPa, and a space velocity of 1000 mL/g_{cat}/h, the H-ZSM-5-25 catalyst achieves an aromatics selectivity of up to 60.2% with a corresponding C_3H_8 conversion of 48.8%. Mechanistic investigations indicate that both lactone species and olefins serve as crucial intermediates in the aromatization pathway. Notably, carbon atoms from CO_2 are incorporated directly into the aromatic ring through these intermediates, circumventing the conventional RWGS route. This innovative pathway opens new horizons for the catalytic synthesis of aromatics and highlights the potential for carbon-neutral chemical production technologies.

2. Experimental

2.1. Catalyst information

The ZSM-5, ZSM-11, ZSM-22, ZSM-23 and ZSM-35 were purchased from Nankai University Catalyst Company. The ZSM-5 samples were named as H-ZSM-5-*X* and *X* represents the ratio of SiO_2/Al_2O_3. Na-zeolites were converted into its NH_4^+ form by exchanging 10 g Na-zeolites with 0.1 L NH_4NO_3 (1 mol/L) aqueous solution at 353 K for 2 h, followed by filtration and washing with deionized water. After repeating the above-mentioned process three times, the desired sample was dried at 383 K for 10 h, followed by calcination at 823 K for another 4 h in air to obtain the H-zeolites catalyst (detected by X-ray fluorescence (XRF)).

2.2. Catalyst characterization

The crystalline structure of the zeolite samples was examined by X-ray diffraction (XRD) on a PANalytical X'Pert PRO instrument using Cu K_α (λ = 0.151 nm) radiation operated at 40 kV and 40 mA. Morphological features were investigated via scanning electron microscopy (SEM) using a Hitachi SU8020 system. Elemental composition was analyzed through XRF on a Philips Magix-601 spectrometer. Acidity was evaluated using NH_3-temperature-programmed desorption (NH_3-TPD) performed on a Micromeritics AutoChem 2920 equipped with a thermal conductivity detector (TCD). Approximately 0.1–0.15 g of sample was loaded into a U-shaped quartz reactor, pretreated in helium at 823 K for 30 min, followed by NH_3 adsorption at 423 K. After purging physisorbed NH_3, desorption was carried out from 423 to 923 K at a ramp rate of 10 K/min under He flow. Textural parameters of the zeolites with different framework structures were derived from N_2 adsorption-desorption isotherms at 77 K.

The temperature-programmed surface reaction of propane was performed in a U-shaped quartz tube connected with a downstream gas sampling mass spectrometer. Thereinto, helium was employed as the carrier gas. 0.15 g catalyst was loaded into U-shaped tube. After pretreating on 823 K for 30 min in He, the temperature was cooled down to 323 K. The gas containing and 95% argon was continuously introduced into the catalyst bed with increasing reaction temperature from 323 to 873 K. The online gas products were detected by MS. Thereinto, the *m*/*z* values of reactants and products were referred as follows: methane (16), ethene (25), propane (44), propylene (42), benzene (78), toluene (92), xylene (106).

The ^{13}C nuclear magnetic resonance (NMR) spectra of products were collected on a Bruker Avance Ⅲ HD 700 MHz spectrometer equipped with a 9.40 T wide-bore magnet. The resonance frequencies were set up at 176.0 MHz for ^{13}C. Approximately 0.25 mL of $CDCl_3$ was dissolved with 0.25 mL samples in an NMR tube. ^{13}C NMR spectra were recorded using high-power proton decoupling. A fixed scans were collected with a π/2 pulse of 12.6 μs and a 2 s recycle delay. The organic species of spent catalysts were analyzed by GC-MS. Specifically, 0.05 g spent zeolite catalysts were dissolved in 0.05 mL HF solution (20%). After being neutralized with 5 wt% NaOH solution, the soluble cokes were extracted with 1 mL CH_2Cl_2 containing 10 mg/L C_2Cl_6 (internal standard) and then analyzed using a GC-MS (Agilent 7890B) instrument with an HP-5 capillary column.

2.3. Catalyst testing

The co-conversion of CO_2 and C_3H_8 was conducted in a stainless-steel fixed-bed reactor (inner diameter 7 mm) designed for high-pressure operations. A measured quantity of catalyst (20–40 mesh), uniformly blended with quartz sand of similar particle size, was packed into the reactor. Prior to the

reaction, the catalyst was activated at 673 K under a nitrogen flow (40 mL/min) for 3 h to eliminate residual moisture from both the zeolite and reactor system. The temperature was then increased to 723 K before introducing the reactant mixture containing CO_2 and C_3H_8 at a controlled pressure. The data was used under near-equilibrium conditions. Product analysis was performed using an Agilent 7890A online gas chromatograph equipped with a flame ionization detector (FID) and a PLOT-Q capillary column for effective separation. Propane conversion and product selectivity were determined based on carbon molar fractions.

$$\text{Conv } C_3H_8 = \frac{\sum_1^n nC_nH_m - 3C_3H_{8\text{outlet}}}{\sum_1^n nC_nH_{m\text{outlet}}} \times 100\%$$

$$\text{Conv } CO_2 = \frac{CO_{2\text{inlet}} - CO_{2\text{outlet}}}{CO_{2\text{inlet}}} \times 100\%$$

$$\text{Sel Product } X = \frac{nC_nH_{m\text{product}}}{\sum_1^n nC_nH_{m\text{outlet}} - 3C_3H_{8\text{outlet}}} \times 100\%$$

$nC_nH_{m\text{outlet}}$: carbon atoms of $C_nH_{m\text{outlet}}$ at the outlet
$3C_3H_{8\text{outlet}}$: carbon atoms of $C_3H_{8\text{outlet}}$ at the outlet
$CO_{2\text{inlet}}$: moles of CO_2 at the inlet
$CO_{2\text{outlet}}$: moles of CO_2 at the outlet
$nC_nH_{m\text{ product}}$: carbon atoms of Product X_{outlet} at the outlet

2.4. *Operando dual-beam Fourier transform infrared spectra (DB-FTIR)*

In order to understand the mechanism deeply, the operando DB-FTIR were carried out on a Nicolet IS50 equipped with a MCT detector, using an operando DB-FTIR cell with ZnSe windows [26]. Firstly, 15 mg of H-ZSM-5-25 was placed in the operando DB-FTIR cell. And then the sample was calcined in an N_2 stream at 673 K for 1 h. Afterwards, the temperature decreased to 423 K in the N_2 stream and the initial background spectrum was recorded. The stream of mixed gas (0.5% C_3H_8, 99.5% Ar) or (0.5% C_3H_8, 49.5% CO_2, 50% Ar) at 10 mL/min was introduced into the cell at 1.0 MPa, which the reaction temperature increased from 423 to 723 K. Moreover, IR spectra from the sample beam and background reference beam were recorded simultaneously. The final information of surface group was obtained by subtraction of the background reference spectra from sample spectra.

2.5. *^{13}C Isotope tracing experiments*

In order to further confirmed reaction mechanism, we carried out the ^{13}C isotope tracing experiments. 0.3 g H-ZSM-5-25 was loaded into reactor. The catalyst was first pretreated at 673 K for 3 h with N_2 gas flow (40 mL/min) and the temperature rose to 723 K. The mixed gas 1 (0.5% C_3H_8, 99.5% Ar) and gas 2 (50% $^{13}CO_2$, 50% Ar) were introduced into reactor with a constant flow. The products were collected by CH_2Cl_2 for 2 h and analyzed by GC-Q-TOF (Agilent 8890-7250) equipped HP-5 column. Moreover, the collected sample was analyzed by ^{13}C liquid-state NMR.

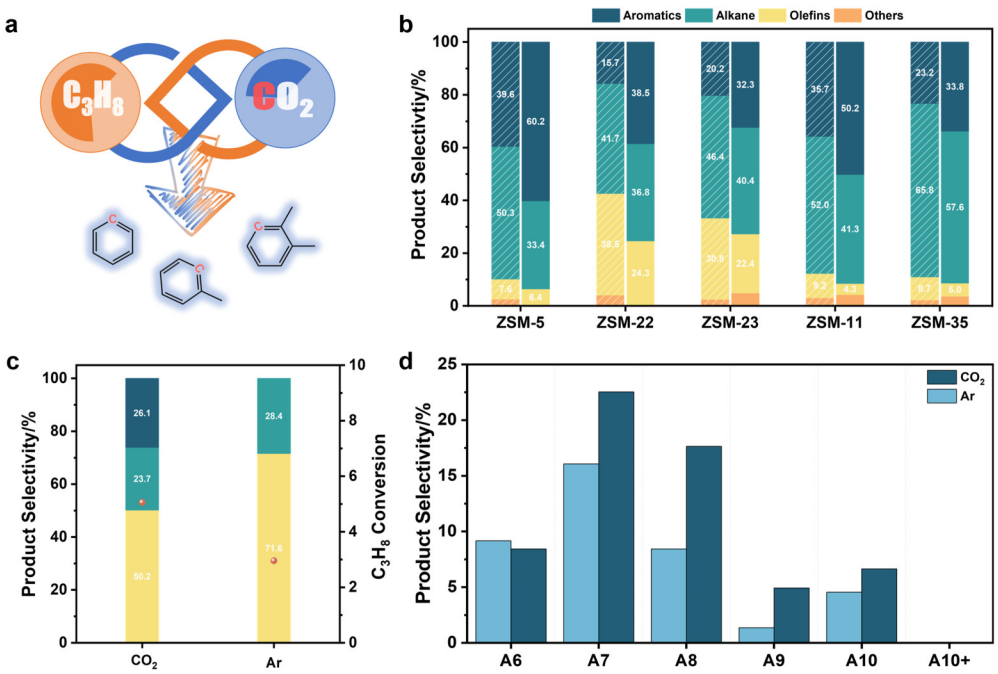

Fig. 1. CO_2-C_3H_8 co-conversion to aromatics over acidic zeolites with varied framework structures. (a) Schematic illustration of the co-conversion strategy. (b) Catalytic performances of different zeolitic topologies in propane aromatization, with and without CO_2 co-feeding. (c) Propane conversion and product distribution over H-ZSM-5 at 0.1 MPa under various gas atmospheres. (d) Aromatic selectivity profiles over H-ZSM-5 at 3.0 MPa under different reaction environments. Reaction conditions: (b,d) 723 K, 20 kPa C_3H_8, (2570 kPa CO_2, 410 kPa Ar solid) or (2980 kPa Ar dash), 1000 mL/g_{cat}/h; (c) 723 K, 0.72 kPa C_3H_8, (86.85 kPa CO_2, 13.43 kPa Ar) or (100.28 kPa Ar), 1000 mL/g_{cat}/h. Note that olefins represent $C_2^=$–$C_4^=$, alkanes represent C_1–C_4^0 (apart from C_3H_8), and others represent C_{5+} hydrocarbon excluding aromatics.

3. Results and discussion

3.1. The coupling effect in the reaction of CO_2 and C_3H_8 over acidic zeolite with different topologies

In this study, a reaction pathway involving the co-transformation of hydrogen-deficient CO_2 and hydrogen-rich C_3H_8 into aromatics was adopted, as illustrated in Fig. 1(a). A series of acidic zeolites, including the topology of MFI, TON, MTT, MEL, and FER, were employed to verify the feasibility of the strategy. Figs. S1–S4 and Table S1 detail the structural and compositional features of the zeolite catalysts. Fig. 1(b) compares product selectivity over different acidic zeolites in the presence and absence of CO_2 under 3.0 MPa, 723 K, and 1000 mL/g_{cat}/h. An obvious increase in aromatics selectivity and decrease in alkane selectivity were simultaneously observed over all acidic zeolites after introducing CO_2 into the conversion of C_3H_8. Specifically, the selectivity to aromatics increased from 39.6% to 60.2%, while the selectivity to alkane selectivity decreased from 50.3% to 33.4%. Besides, aromatics selectivity increased by 22.8%, 12.1%, 14.3%, and 10.6% over ZSM-22, ZSM-23, ZSM-11, and ZSM-35, respectively. These observations suggested that the coupling conversion reaction strategy was feasible. Moreover, the change of product distribution was different from the traditional propane aromatization reaction, indicating that a new aromatization mechanism might exist. Furthermore, the CO_2-C_3H_8 co-conversion to aromatics over H-ZSM-5 was carried out at 0.1 MPa (Fig. 1(c)). A large amount of ethylene (53.4%) and methane (27.8%) was observed and aromatics was not detected under Ar atmosphere. Meanwhile, the selectivity to aromatics increased by 26.1% and the alkane and olefins selectivity decreased simultaneously. Additionally, the detailed aromatics selectivity exhibited varying degrees of improvement (Fig. 1(d)). Thereinto, the selectivity of toluene and xylene increased by 6.5% and 9.2%, respectively. These results further confirmed that the aromatization process of C_3H_8 was obviously promoted after introducing CO_2. Remarkably, the C_3H_8 conversion increased from 3.0% to 5.1% at 0.1 MPa after introducing CO_2 (Fig. 1(c)). The above results indicate that CO_2 incorporation simultaneously enhances C_3H_8 conversion and selectivity toward aromatics. Moreover, the pathway for aromatic formation may also be altered in the presence of CO_2.

3.2. The influence of SiO_2/Al_2O_3 ratio in H-ZSM-5 on CO_2-C_3H_8 coupling aromatization

The acidic properties of zeolite, such as SiO_2/Al_2O_3, was important factor affecting the catalytic performance [27]. H-ZSM-5, as the most efficient catalyst, was used to investigate the influence of acid amounts on the conversion of CO_2 and C_3H_8. The structural features and acidity characteristics of the catalysts are summarized in Figs. S1–S4 and Table S1. As illustrated in Fig. 2(a), the product selectivity over H-ZSM-5 with varying SiO_2/Al_2O_3 ratios was evaluated under CO_2 and Ar atmospheres. When the SiO_2/Al_2O_3 ratio increased from 25 to 145, the selectivity toward aromatics declined from 60.2% to 40.2% under CO_2, and from 39.6% to 17.9% under Ar. These results highlight the essential role of Brönsted acidity, indicating that the co-conversion of CO_2 and C_3H_8 proceeds through a typical acid-catalyzed pathway. As shown in Figs. 2(a) and S5, under Ar atmosphere, the aromatics selectivity and alkane selectivity simultaneously increase with increasing Al content. This result was consistent with the traditional C_3H_8 aromatization [28]. Specifically, the acidity of zeolites primarily governs dehydrogenation, oligomerization, and hydrogen transfer steps. Nevertheless, in comparison with the reaction under an Ar atmosphere, the introduction of CO_2 notably promotes aromatic formation during the co-conversion with C_3H_8 over H-ZSM-5 catalysts with increasing aluminum content, accompanied by a marked reduction in alkane selectivity. As illustrated in Fig. 2(b), aromatics selectivity was positively corrected with Al content, while alkane selectivity and olefins selectivity were negatively correlated inconsistent with hydrogen transfer mechanism to synthesize aromatics. Obviously, the acidity of zeolites plays a distinct role in the coupling conversion of CO_2 and C_3H_8. Therefore, we deduced that the improvement of aromatics was strongly dependent on the Al content and CO_2. Moreover, CO_2 might be involved in the formation of aromatics.

3.3. The influence of reaction parameters on CO_2-C_3H_8 coupling aromatization over H-ZSM-5-25

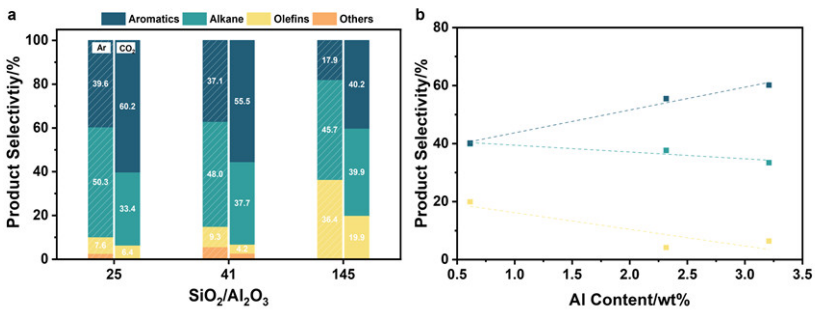

Fig. 2. Catalytic behavior of H-ZSM-5 catalysts with varying SiO_2/Al_2O_3 ratios on the co-conversion of CO_2 and C_3H_8. (a) Selectivity distribution of main products. (b) Correlation between aluminum content in H-ZSM-5 and the selectivity toward aromatics, alkanes, and olefins. Reaction conditions: (a) 723 K, 20 kPa C_3H_8, (2570 kPa CO_2, 410 kPa Ar) or (2980 kPa Ar), 1000 mL/g_{cat}/h; (b) 723 K, 20 kPa C_3H_8, 2570 kPa CO_2, 410 kPa Ar, 1000 mL/g_{cat}/h; Note that olefins represent $C_2^=$–$C_4^=$, alkanes represent C_1–C_4^0 (apart from C_3H_8), and others represent C_{5+} hydrocarbon excluding aromatics.

As shown in Fig. 3(a), the total reaction pressure exerts a significant effect on the co-conversion of CO_2 and C_3H_8 over H-ZSM-5-25. With pressure elevated from 0.1 to 4.0 MPa, aromatic selectivity notably increased from 26.1% to 59.9%. Moreover, alkane selectivity increased by ca.10% gradually and the selectivity to olefins dramatically decreased by 44.2%. C_3H_8 conversion also significantly increased by 46.1%. Thereinto, C_3H_8 conversion and aromatics selectivity reached 40% and ca. 60%, respectively. These observations indicated that the higher reaction pressure is beneficial for the co-conversion of CO_2 and C_3H_8 to aromatics. As exhibited in Fig. 3(b), a linear increase in C_3H_8 conversion and a volcanic change trend of aromatic and alkane selectivity were discovered with the increase of reaction temperature. 24.7% C_{5+} selectivity was observed at 573 K and disappeared with increasing reaction temperature, which was inconsistent with traditional aromatics formation route. Evidently, elevated reaction temperatures promoted C_3H_8 conversion, which in turn favored the formation of aromatics.

Fig. 3(c) illustrates that the partial pressure of CO_2 had a pronounced influence on its co-conversion with C_3H_8. As the CO_2 partial pressure increased, the selectivity toward aromatics rose steadily from 51.1% to 60.2%, while the selectivity for alkanes and olefins declined from 37.8% to 33.4% and from 9.1% to 6.4%, respectively. More importantly, the ratio of converted CO_2 and C_3H_8 increased linearly with increasing CO_2 partial pressure. Thereinto, the conversion amount of C_3H_8 was close. It can be concluded that increasing CO_2 partial pressure was conducive to the conversion of CO_2. Furthermore, CO can only be detected at a CO_2 pressure of 2.57 MPa (~5.1% CO selectivity). It also meant that almost the converted CO_2 was transformed into aromatics. These above results directly confirmed that the coupling effect between CO_2 and C_3H_8 existed over zeolite catalyst. Furthermore, the low ratio of CO_2/C_3H_8 has also been investigated by adjusting reaction conditions, as shown in Fig. S6. With increasing the ratio of CO_2/C_3H_8, the selectivity to aromatics increased obviously while alkanes selectivity decreased, which is different from the traditional hydrogen transfer mechanism. These findings provide additional evidence supporting the presence of a distinct aromatization pathway involved in the co-conversion of CO_2 and C_3H_8.

The influence of contact times on the catalytic performance was illustrated in Fig. 3(d). As contact times increased, the olefins selectivity sharply decreased from 21.6% to 6.4% and the aromatics selectivity increased from 51.4% to 60.2%. Additionally, with prolonging the contact times, the C_3H_8 conversion linearly increased from 9.1% to 48.8%. Therefore, combing with the results of Figs. 3(c) and (d), aromatics might be produced from olefins and CO_2 and prolonging contact times was beneficial for the coupling conversion of CO_2 and C_3H_8. Remarkably, the slow increase of alkane selectivity also indicated a new aromatization mechanism different from hydrogen transfer mechanism might exist.

3.4. The reaction mechanism of the CO_2-C_3H_8 coupling aromatization

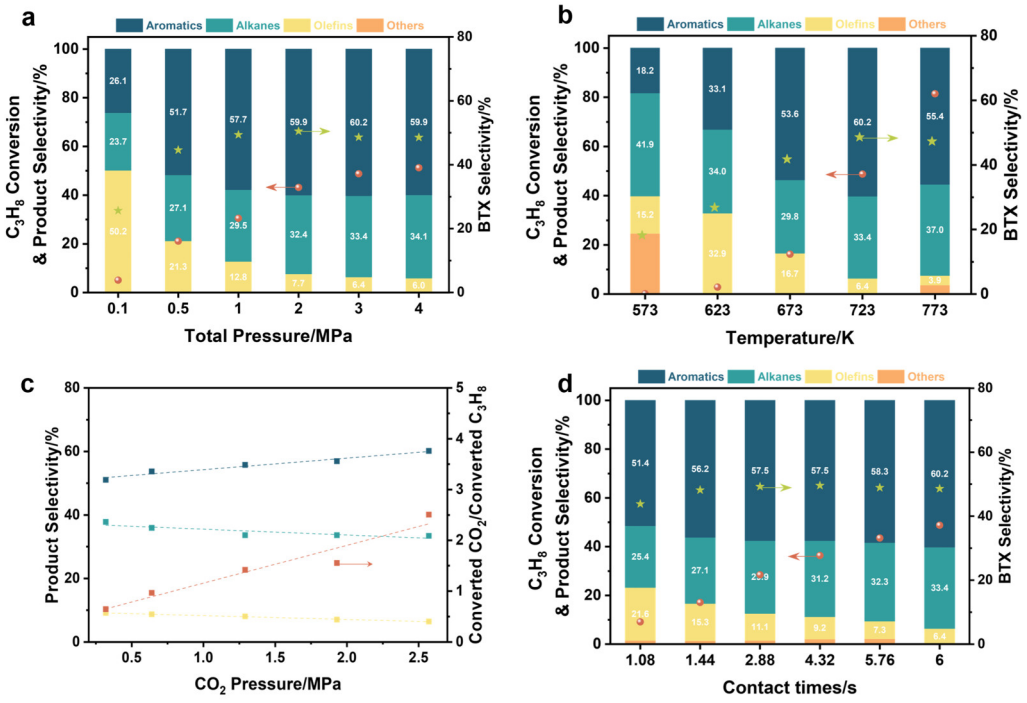

Fig. 3. Impact of reaction parameters on the co-conversion of CO_2 and C_3H_8 over H-ZSM-5-25. (a) Variation in propane conversion and product distribution with total reaction pressure. (b) Dependence of C_3H_8 conversion and product selectivity on reaction temperature. (c) Effect of CO_2 partial pressure on selectivity trends and converted CO_2/ C_3H_8 ratios. (d) Product profile and propane conversion as a function of contact time. Reaction conditions: (a) 723 K, C_3H_8:CO_2 = 1:120, 1000 mL/g_{cat}/h; (b) 20 kPa C_3H_8, 2570 kPa CO_2, 410 kPa Ar, 1000 mL/g_{cat}/h; (c) 723 K, 20 kPa C_3H_8, 0–2570 kPa CO_2, 1000 mL/g_{cat}/h, Ar as balance gas; (d) 723 K, 20 kPa C_3H_8, 2570 kPa CO_2, 410 kPa Ar. Note that olefins represent $C_2^=$–$C_4^=$, alkanes represent C_1–C_4^0 (apart from C_3H_8), and others represent C_{5+} hydrocarbon excluding aromatics.

To gain insight into the coupling mechanism between CO_2 and C_3H_8, product distributions as a function of contact time are presented in Fig. 4(a). As contact time increased, the selectivity of ethylene and propylene gradually declined, while butene selectivity initially rose and subsequently decreased. Moreover, methane selectivity maintained at ca. 18%. These results indicated that C_3H_8 might be cracked to produce ethylene and methane at the beginning of the reaction. Whereafter, ethylene was oligomerized to butene and then converted to aromatics. To further confirm this point, the temperature-programmed surface reaction of propane over H-ZSM-5-25 has been carried out, as shown in Fig. S7. Obviously, the conversion of C_3H_8 was difficult to occur below 673 K. As the reaction temperature continued to rise, the intensities of methane and ethylene signals exhibited a progressive increase. Whereafter, the signal of propylene slowly increased. These observations indicated that propane was preferentially cracked to methane and ethylene. Therefore, the cracking of propane is an important step for the coupling of CO_2 and C_3H_8. To clarify the role of olefins, different olefins, such as ethylene, propylene and butene, were employ under the same conditions (Fig. S8). Obviously, after introducing CO_2 into C_3H_8, the aromatics selectivity can be enhanced while the selectivity to alkanes decreased. These findings further suggest that olefins may participate in a CO_2-involved pathway leading to the improvement of aromatics formation.

Furthermore, the residual species were captured at different contact times, which were analyzed by GC-MS (Fig. 4(b) and S9). Lactone species and aromatics species were observed, exhibiting a volcanic type change trend. Obviously, these species changed synchronously with the prolonging of contact time, which were consistent with the change of aromatics selectivity in the product. In our previous work [21,23], it has been proven that γ-valerolactone can be produced from olefins and CO_2. To further confirm the role of lactones, γ-valerolactone was selected as probe molecule pre-absorbed on H-ZSM-5-25, which was converted at different reaction temperature. The residual species trapped in spent catalysts were analyzed by GC-MS, as shown in Fig. S10 [23]. With the increase of reaction temperature, γ-valerolactone gradually decreased and the cyclopentenone showed a volcanic type change trend. Moreover, aromatics species, such as toluene and xylene, increased gradually. The results confirmed that γ-valerolactone undergoes transformation to cyclopentenone, contributing to aromatic formation. Based on this, it is proposed that C_3H_8 may first convert into light olefins, which subsequently interact with CO_2 to generate lactone intermediates, ultimately leading to the production of aromatics.

To further clarify the coupling reaction mechanism, operando DB-FTIR spectra were employed over H-ZSM-5 at different reaction temperature. Fig. 4(c) (down) exhibited the evolution of surface species for the conversion of C_3H_8 to aromatics over H-ZSM-5-25. With increasing reaction temperature from 423 to 723 K, the negative band at 3608 cm^{-1} assigned to Si(OH)Al gradually decreased. The band at 2983, 2965, 2901, and 2872 cm^{-1} were observed, which were attributed to the surface alkoxy groups [29,30]. Simultaneously, a slow increase for the intensity of the peaks C=C of olefins (1658 cm^{-1}) and aromatics (1508 and 1486 cm^{-1}) was discovered [31–33]. These results indicated that C_3H_8 was first absorbed at the Brönsted acidic sites, which then form olefins and finally aromatic. After introducing CO_2 into the conversion of C_3H_8 conversion, as shown in Fig. 4(c) (up), the new peaks at 3729, 3697, 3626, and 3596 cm^{-1} appeared attributing to the CO_2 gas [23]. Additionally, the new peaks at 1746, 1681, and 1562 cm^{-1}

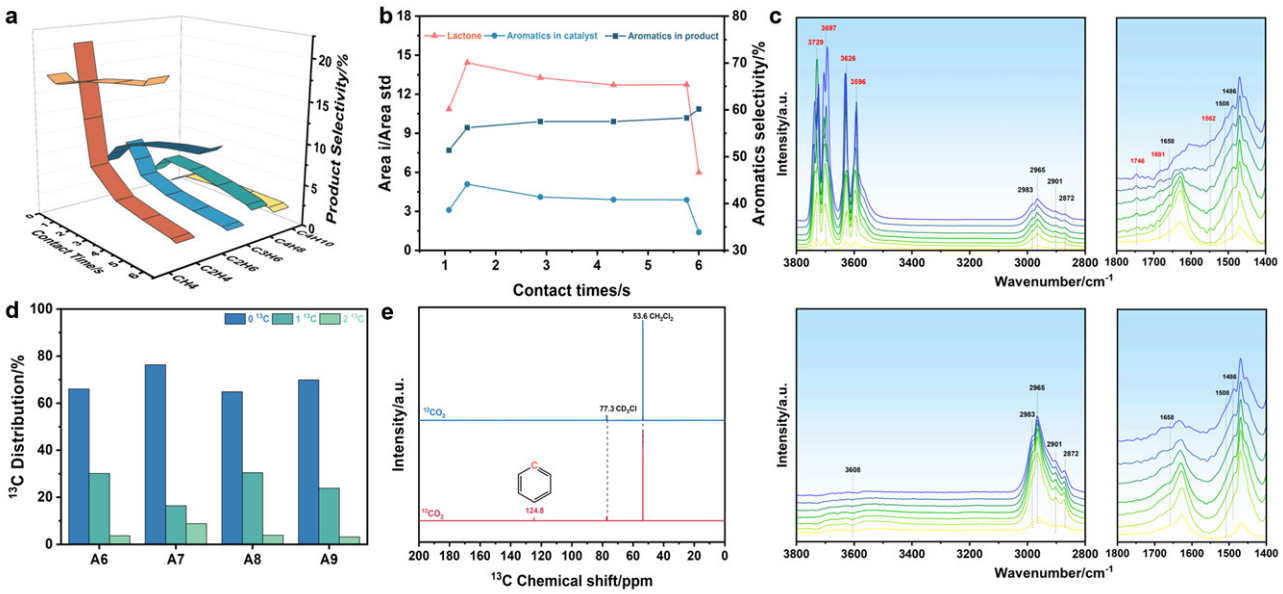

Fig. 4. Mechanistic investigation of the CO_2-C_3H_8 co-conversion over H-ZSM-5-25. (a) Correlation between contact time and light hydrocarbon formation. (b) Effect of contact time on residual surface species and aromatic selectivity. (c) Operando dual-beam FTIR spectra of propane conversion under different gas atmospheres. (d) ^{13}C isotope distribution in aromatic products. (e) ^{13}C liquid-state NMR spectra of products derived from the coupling reaction between $^{13}CO_2$ and C_3H_8. Reaction conditions: (a,b) 723 K, 20 kPa C_3H_8, 2570 kPa CO_2, 410 kPa Ar; (c) 423–723 K, 1.0 MPa, C_3H_8:CO_2 = 1:99 (up), C_3H_8 : Ar = 1:99 (down), 40000 mL/g_{cat}/h; (d,e) 723 K, 1.5 kPa C_3H_8, 500 kPa CO_2, 798.5 kPa Ar, 1300 mL/g_{cat}/h.

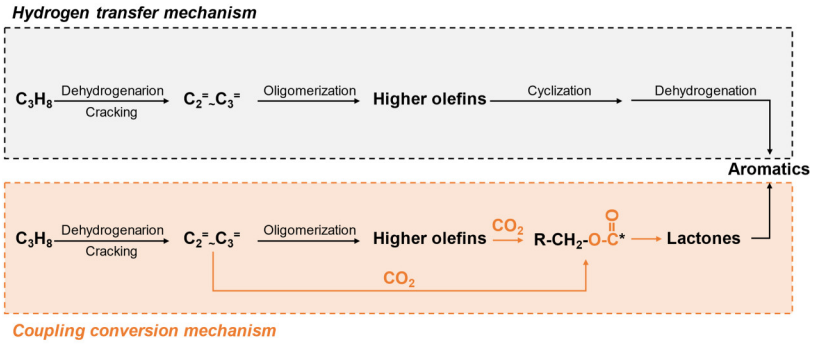

Fig. 5. Schematic illustration of the CO_2-C_3H_8 coupling aromatization over H-ZSM-5.

can be assigned to the C=O of lactones species, ketone species, and carbonate species [13,32,34,35], respectively. Thereinto, the intensity of carbonate species exhibited a volcano change trend, and the lactones and ketones species increased gradually with increasing reaction temperature. At the same time, the sign of aromatics also increased. In our previous work, it can be confirmed that olefins and CO_2 can be transformed into lactones and then form aromatics [23]. Therefore, we thought that C_3H_8 can be cracked to produce ethylene, which can oligomerize and react with CO_2 to form lactones and eventually aromatics.

To directly verify the interaction between CO_2 and C_3H_8, a ^{13}C isotopic labeling experiment was conducted under conditions of 723 K, 1.3 MPa, and a space velocity of 1300 mL/g_{cat}/h. As shown in Fig. 4(d), the ^{13}C-labeled products, extracted using CH_2Cl_2 and analyzed by GC-MS, reveal the carbon distribution resulting from the reaction of $^{13}CO_2$ with C_3H_8. Obviously, benzene, xylene, toluene, and trimethylbenzene all contained ^{13}C atom, which indicated that CO_2 participated in the formation of aromatics. According to our previous work, the aromatics containing two ^{13}C might be produced by $^{13}CO_2$ and ^{13}C-olefins. Furthermore, the ^{13}C liquid NMR has been used to verify the site of ^{13}C atom in the product, as shown in Fig. 4(e). The peak at 124.8 δ, which was attributing to the C atom in the aromatic ring [36,37]. Moreover, no signal is observed at corresponding chemical shift with the feeding of $^{12}CO_2$ and C_3H_8. This observation directly demonstrated that CO_2 can be selectivity incorporated into the aromatic ring and the coupling effect between CO_2 and C_3H_8 existed.

According to the above results, the novel C_3H_8 aromatization mechanism under CO_2 atmosphere was proposed, as shown in Fig. 5. C_3H_8 first adsorbed at Brönsted acidic sites and cracked to ethylene or dehydrogenation to propylene. The light olefins can oligomerize to produce higher olefins. The formed olefins can react with CO_2 to form carbonate species, which were converted to lactones and eventually aromatics. The coupling conversion mechanism realized H/C balance between reactants and products inhibiting the formation of alkane, which effectively improves the aromatics selectivity.

4. Conclusions

In summary, we established a transformative strategy for propane aromatization by enabling the dual role of CO_2 as both a hydrogen regulator and a carbon donor. It was demonstrated that the introduction of CO_2 significantly enhances both the conversion of C_3H_8 and the formation of aromatics. Under the conditions of 723 K, 3.0 MPa, and a space velocity of 1000 mL/g_{cat}/h, co-feeding CO_2 with C_3H_8 over H-ZSM-5-25 led to an aromatic selectivity of approximately 60% and a C_3H_8 conversion of about 48%. Combined insights from operando dual-beam FTIR spectroscopy and ^{13}C isotope-labeling experiments revealed that olefins and lactone intermediates play essential roles in the co-conversion pathway. Notably, the carbon atoms from CO_2 were directly incorporated into the aromatic ring structures, bypassing the conventional reverse water-gas shift route reported in previous studies. This innovative pathway opens new horizons for the catalytic synthesis of aromatics and highlights the potential for carbon-neutral chemical production technologies.

Electronic supporting information

Supporting information is available in the online version of this article.

Competing interests

Authors declare that they have no competing interests.

References

[1] B. M. Tackett, E. Gomez, J. G. Chen, *Nat. Catal.*, **2019**, 2, 381–386.
[2] T. Sakakura, J.-C. Choi, H. Yasuda, *Chem. Rev.*, **2007**, 107, 2365–2387.
[3] C. Hepburn, E. Adlen, J. Beddington, E. A. Carter, S. Fuss, N. Mac Dowell, J. C. Minx, P. Smith, C. K. Williams, *Nature*, **2019**, 575, 87–97.
[4] G. Tian, X. Liang, H. Xiong, C. Zhang, F. Wei, *EES Catal.*, **2023**, 1, 677–686.
[5] D. Wang, Z. Xie, M. D. Porosoff, J. G. Chen, *Chem*, **2021**, 7, 2277–2311.
[6] R.-P. Ye, J. Ding, W. Gong, M. D. Argyle, Q. Zhong, Y. Wang, C. K. Russell, Z. Xu, A. G. Russell, Q. Li, M. Fan, Y.-G. Yao, *Nat. Commun.*, **2019**, 10, 5698.
[7] S. Dabral, T. Schaub, *Adv. Synth. Catal.*, **2019**, 361, 223–246.
[8] A. Behr, *Chem. Ing. Tech.*, **1985**, 57, 893–903.

Graphical Abstract

Chin. J. Catal., 2025, 72: 314–322 doi: 10.1016/S1872-2067(25)64680-8

Efficient carbon integration of CO_2 in propane aromatization over acidic zeolites

Cheng Li, Xudong Fang *, Bin Li, Siyang Yan, Zhiyang Chen, Leilei Yang, Shaowen Hao, Hongchao Liu, Jiaxu Liu *, Wenliang Zhu *
Dalian Institute of Chemical Physics, Chinese Academy of Sciences;
University of Chinese Academy of Sciences;
Dalian University of Technology

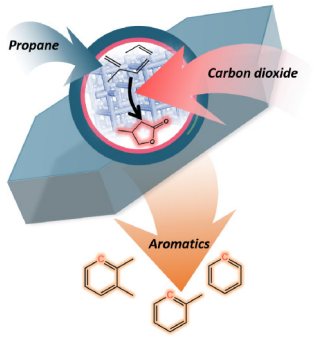

An efficient strategy converting CO_2 and C_3H_8 *via* a coupling aromatization mechanism involving olefins and lactones has been reported, enabling direct incorporation of CO_2 into aromatic rings and thus achieving high carbon utilization.

[9] S. Fukuoka, M. Kawamura, K. Komiya, M. Tojo, H. Hachiya, K. Hasegawa, M. Aminaka, H. Okamoto, I. Fukawa, S. Konno, *Green Chem.*, **2003**, 5, 497–507.
[10] M. A. Pacheco, C. L. Marshall, *Energy Fuels*, **1997**, 11, 2–29.
[11] Y. Wang, X. Gao, M. Wu, N. Tsubaki, *EcoMat*, **2021**, 3, e12080.
[12] A. Ramirez, A. Dutta Chowdhury, A. Dokania, P. Cnudde, M. Caglayan, I. Yarulina, E. Abou-Hamad, L. Gevers, S. Ould-Chikh, K. De Wispelaere, V. van Speybroeck, J. Gascon, *ACS Catal.*, **2019**, 9, 6320–6334.
[13] S. Wang, L. Zhang, P. Wang, X. Liu, Y. Chen, Z. Qin, M. Dong, J. Wang, L. He, U. Olsbye, W. Fan, *Chem*, **2022**, 8, 1376–1394.
[14] J. Zuo, W. Chen, J. Liu, X. Duan, L. Ye, Y. Yuan, *Sci. Adv.*, **2020**, 6, eaba5433.
[15] X. Niu, X. Nie, C. Yang, J. G. Chen, *Catal. Sci. Technol.*, **2020**, 10, 1881–1888.
[16] S.-K. Ihm, Y.-K. Park, S.-W. Lee, *Appl. Organometal. Chem.*, **2000**, 14, 778–782.
[17] J.-B. Zhang, H.-H. He, H.-F. Tian, J.-K. Liao, F. Zha, X.-J. Guo, X. Tang, Y. Chang, *Can. J. Chem.*, **2021**, 99, 619–627.
[18] H. Fan, X. Nie, C. Song, X. Guo, *Ind. Eng. Chem. Res.*, **2022**, 61, 10483–10495.
[19] J. Guo, H. Lou, H. Zhao, L. Zheng, X. Zheng, *J. Mol. Catal. A*, **2005**, 239, 222–227.
[20] K. Bu, Y. Kang, Y. Li, Y. Zhang, Y. Tang, Z. Huang, W. Shen, H. Xu, *Appl. Catal. B*, **2024**, 343, 123528.
[21] C. Wei, W. Zhang, K. Yang, X. Bai, S. Xu, J. Li, Z. Liu, *Chin. J. Catal.*, **2023**, 47, 138–149.
[22] X. Ren, Z.-P. Hu, J. Han, Y. Wei, Z. Liu, *Front. Chem. Sci. Eng.*, **2023**, 17, 1801–1808.
[23] X. Fang, B. Li, H. Liu, M. Xie, Z. Chen, L. Yang, J. Han, W. Zhu, Z. Liu, *Chem Catal.*, **2023**, 3, 100689.
[24] M. Guisnet, S. N. Gnep, D. Aittaleb, J. Y. Doyemet, *Appl. Cata. A*, **1992**, 87, 255–270.
[25] Y. Song, Z.-P. Hu, H. Feng, E. Chen, L. Lv, Y. Wu, Z. Liu, Y. Jiang, X. Su, F. Xu, M. Zhu, J. Han, Y. Wei, S. Mintova, Z. Liu, *J. Energy Chem.*, **2024**, 97, 513–519.
[26] J. Liu, J. Wang, W. Zhou, C. Miao, G. Xiong, Q. Xin, H. Guo, *Chin. J. Catal.*, **2017**, 38, 13–19.
[27] Q. Zhang, J. Yu,A. Corma, *Adv. Mater.*, **2020**, 32, 2002927.
[28] L. Lin, J. Liu, X. Zhang, J. Wang, C. Liu, G. Xiong, H. Guo, *Ind. Eng. Chem. Res.*, **2020**, 59, 16146–16160.
[29] J. A. van Bokhoven, M. Tromp, D. C. Koningsberger, J. T. Miller, J. A. Z. Pieterse, J. A. Lercher, B. A. Williams, H. H. Kung, *J. Catal.*, **2001**, 202, 129–140.
[30] I. I. Ivanova, E. B. Pomakhina, A. I. Rebrov, E. G. Derouane, *Top. Catal.*, **1998**, 6, 49–59.
[31] E. D. Hernandez, F. C. Jentoft, *ACS Catal.*, **2020**, 10, 5764–5782.
[32] J.-Y. Zhou, G.-D. Lu, S.-H. Wu, *Synth. Commun.*, **1992**, 22, 481–487.
[33] X. Fang, H. Liu, Z. Chen, Z. Liu, X. Ding, Y. Ni, W. Zhu, Z. Liu, *Angew. Chem. Int. Ed.*, **2022**, 61, e202114953.
[34] Z. Zhou, H. Liu, Y. Ni, F. Wen, Z. Chen, W. Zhu, Z. Liu, *J. Catal.*, **2021**, 396, 360–373.
[35] C. Lievens, D. Mourant, M. He, R. Gunawan, X. Li, C.-Z. Li, *Fuel*, **2011**, 90, 3417–3423.
[36] Z. Chen, Y. Ni, Y. Zhi, F. Wen, Z. Zhou, Y. Wei, W. Zhu, Z. Liu, *Angew. Chem. Int. Ed.*, **2018**, 57, 12549–12553.
[37] C. Wei, J. Li, K. Yang, Q. Yu, S. Zeng, Z. Liu, *Chem Catal.*, **2021**, 1, 1273–1290.

酸性分子筛上CO_2与丙烷制芳烃中碳原子高效利用

李 诚[a,b], 房旭东[a,*], 李 斌[a,b], 闫思杨[c], 陈之旸[a], 杨磊磊[a,b], 郝邵雯[a,b], 刘红超[a], 刘家旭[c,*], 朱文良[a,*]

[a]中国科学院大连化学物理研究所, 低碳催化国家工程研究中心, 辽宁大连116023
[b]中国科学院大学, 北京100049
[c]大连理工大学化工学院, 精细化工国家重点实验室, 智能材料前沿科学中心, 辽宁大连116012

摘要: 芳烃作为现代工业体系的关键基础化学品, 在合成树脂、纤维、医药等领域应用广泛. 传统石油基生产路线高度依赖石脑油催化重整, 面临石油资源短缺与碳排放双重压力. 与此同时, CO_2作为典型温室气体, 其资源化利用兼具减排与碳

资源高效转化的战略价值, 但受限于其热力学稳定性, 通过加氢路径高选择性制芳烃仍存在挑战. 丙烷作为天然气、页岩气的主要成分, 直接芳构化时因碳氢比失衡导致大量小分子烷烃副产物生成, 限制了芳烃选择性. 因此, 开发CO_2与丙烷耦合转化制芳烃新路线, 突破碳氢限制, 定向提高芳烃选择性, 实现低碳烷烃资源高值化利用, 对构建绿色低碳的芳烃生产技术体系具有重要科学意义和工业应用潜力.

本文创新性地提出酸性分子筛催化CO_2与丙烷耦合定向转化制芳烃的新策略. 选用具有十元环孔道结构的H-ZSM-5分子筛为催化剂, 系统对比了丙烷在Ar/CO_2气氛下的转化行为. 实验结果表明, CO_2的引入显著提升芳烃选择性, 在723 K, 3.0 MPa, C_3H_8/CO_2 = 1:120条件下, 丙烷转化率达48.8%, 芳烃选择性提升至60.2%, 较Ar气氛下提高约30%. 通过调控分子筛Brönsted酸量发现, 提高Brönsted酸量可抑制小分子烷烃生成, 促进丙烷向芳烃的定向转化. 这表明CO_2氛围下的丙烷芳构化过程是有异于传统氢转移机理的Brönsted酸催化过程. 通过双光束原位红外光谱、^{13}C同位素标记实验、丙烷程序升温表面反应实验和探针分子实验, 证明了烯烃和内酯是关键中间物种, 且CO_2中的碳原子直接参与芳环形成, 提出了CO_2与丙烷在酸性分子筛上基于烯烃和内酯的耦合转化新机制, 即“丙烷裂解/脱氢→烯烃-CO_2耦合形成内酯→芳烃”的多步反应机制, 其中CO_2通过与烯烃结合调控氢转移过程, 突破传统芳构化反应的碳氢平衡限制.

综上, 本文为CO_2与低碳烷烃耦合制芳烃提供了新思路, 通过揭示含氧中间体介导的反应机制, 深化了对复杂耦合反应过程的理解. 未来可进一步优化分子筛孔道结构与酸性位点分布, 提高芳烃收率. 本工作不仅为石化行业“减油增化”转型提供新的思路, 也为实现CO_2大规模资源化利用和“双碳”目标贡献了催化科学新方案.

关键词: CO_2利用; 丙烷芳构化; 耦合效应; 酸性分子筛; 内酯

收稿日期: 2025-01-24. 接受日期: 2025-03-26. 上网时间: 2025-05-20.

*通讯联系人. 电子信箱: xdfang@dicp.ac.cn (房旭东), liujiaxu@dlut.edu.cn (刘家旭), wlzhu@dicp.ac.cn (朱文良).

基金来源: 国家自然科学基金(22402179, 22472016, 21991094, 21991090); 中国科学院战略先导专项“清洁能源转化技术与示范”(XDA21030100); 大连市高层次人才创新支持计划(2017RD07); 国家高层次人才专项支持计划(SQ2019RA2TST0016).